Vertical length scale selection for pancake vortices in strongly stratified viscous fluids

Ramiro Godoy-Diana, Jean-Marc Chomaz, Paul Billant

Vertical length scale selection for pancake vortices in strongly stratified viscous fluids

By RAMIRO GODOY-DIANA, JEAN-MARC CHOMAZ
AND PAUL BILLANT

LadHyX, CNRS–École Polytechnique, F-91128 Palaiseau Cedex, France

The evolution of pancake dipoles of different aspect ratio is studied in a stratified tank experiment. Two cases are reported here for values of the dipole initial aspect ratio $\alpha_0 = L_v/L_h$ (where L_v and L_h are vertical and horizontal length scales, respectively) of $\alpha_0 = 0.4$ (case I) and $\alpha_0 = 1.2$ (case II). In the first case, the usual decay scenario is observed where the dipole diffuses slowly with a growing thickness and a decaying circulation. In case II, we observed a regime where the thickness of the dipole decreases and the circulation in the horizontal mid-plane of the vortices remains constant. We show that this regime where the vertical length scale decreases can be explained by the shedding of two boundary layers at the top and bottom of the dipole that literally peel off vorticity layers. Horizontal advection and vertical diffusion cooperate in this regime and the decrease towards the viscous vertical length scale $\delta = L_h Re^{-1/2}$ occurs on a time scale $\alpha_0 Re^{1/2} T_A$, T_A being the advection time L_h/U. From a scaling analysis of the equations for a stratified viscous fluid in the Boussinesq approximation, two dominant balances depending on the parameter $R = Re F_h^2$ are discussed, where $F_h = U/N L_h$ is the horizontal Froude number and $Re = U L_h/\nu$ is the Reynolds number, U, N and ν being, respectively, the translation speed of the dipole, the Brunt–Väisälä frequency and the kinematic viscosity. When $R \gg 1$ the vertical length scale is determined by buoyancy effects to be of order $L_b = U/N$. The experiments presented in this paper pertain to the case of small R, where viscous effects govern the selection of the vertical length scale. We show that if initially $L_v \leqslant \delta$, the flow diffuses on the vertical (case I), while if $L_v \gg \delta$ (case II), vertically sheared horizontal advection decreases the vertical length scale down to δ. This viscous regime may explain results from experiments and numerical simulations on the late evolution of stratified flows where the decay is observed to be independent of the buoyancy frequency N.

1. Introduction

The emergence and evolution of pancake vortices in strongly stratified fluids have been studied intensely (see Spedding, Browand & Fincham 1996; Riley & Lelong 2000; Billant & Chomaz 2000*a*; Bonnier, Eiff & Bonneton 2000; Beckers *et al.* 2001; Praud & Fincham 2003) because of their role in the dynamics of geophysical flows. Of particular interest is the vertical length scale selection that constrains the energy and momentum exchanges – which determine for instance the observed horizontal and vertical turbulence spectra observed in the atmosphere (Lindborg 2002) and in the ocean. The vertical length scale naturally emerging in stratified turbulence has sometimes been observed in numerical simulations (e.g. Herring & Métais 1989;
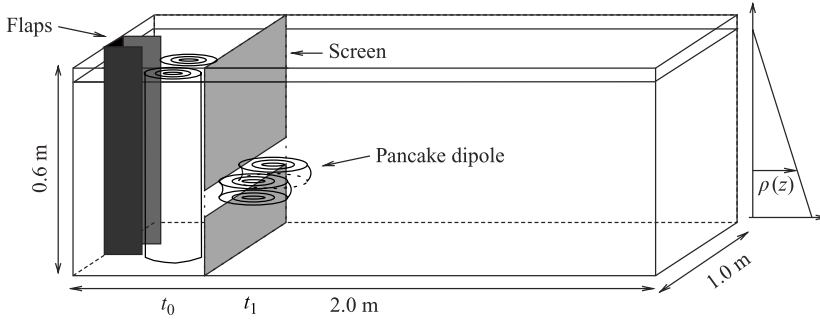
FIGURE 1. Experimental setup.

Kimura & Herring 1996; Riley & deBruynKops 2003) and laboratory experiments (e.g. Fincham, Maxworthy & Spedding 1996; Bonnier *et al.* 2000) to be independent of the strength of the stratification, depending only on the Reynolds number. On the other hand, a dependence on the Brunt–Väisälä frequency, N, of the vertical length scale has been observed in the stratified Taylor–Couette experiment (Boubnov, Gledzer & Hopfinger 1995), in stratified wakes (Park, Whitehead & Gnanadeskian 1994; Holford & Linden 1999; Spedding 2002), in the zigzag instability of a columnar dipole (Billant & Chomaz 2000*a*), in numerical simulations of decaying stratified turbulence (Godeferd & Staquet 2003) and in the vertical wavenumber spectra in the tropopause and lower stratosphere (Lindborg 2002).

In the present paper we study experimentally the dynamics of a pancake dipole in a linearly stratified fluid. The dipole evolves differently depending on its initial aspect ratio. For thin dipoles the vertical length scale grows very slowly while its circulation decays, and the evolution is described well by the constant-thickness model proposed by Flor, van Heijst & Delfos (1995). When the initial dipole is thicker, a new regime is observed where the top and bottom layers of the dipole are 'peeled off' forming a wake so that the dipole is slimmed vertically. From these observations we propose different regimes for the evolution of the vertical length scale in stratified flows.

2. Experimental setup

The experiments are carried out in a tank of $1\,\mathrm{m} \times 2\,\mathrm{m}$ base and $0.6\,\mathrm{m}$ height filled with salt-stratified water. The stratification is made using a two-tank method as explained in Billant & Chomaz (2000*a*, referred to hereafter as BC) . All experiments are conducted with linear stratifications of Brunt–Väisälä frequencies in the range 1.4–$1.6\,\mathrm{rad\,s^{-1}}$. The dipole is generated by a pair of parallel vertical flaps as described in BC. The experimental setup differs from BC in that the initial dipole is partially blocked by a vertical screen perpendicular to the direction of motion of the dipole (figure 1). A single horizontal slice of the vortex column goes through the screen and forms a pancake dipole. This method permits the initial aspect ratio and propagation velocity of the pancake dipole to be varied at will, unlike other generation techniques such as impulsive jets (e.g Flor, van Heijst & Delfos 1995) where the vertical scale is determined by the collapse of an initially turbulent patch and not externally controlled. The screen is placed $0.25\,\mathrm{m}$ away from the edge of the flaps. Three non-dimensional control parameters can be defined for the dipole coming out of the screen: the Reynolds number $Re_0 = U_0 L_{h0}/\nu$, the horizontal Froude number $F_{h0} = U_0/N L_{h0}$ and the aspect ratio $\alpha_0 = L_{v0}/L_{h0}$, where U_0, L_{h0} and L_{v0} are, respectively, the initial

translation speed and the horizontal and vertical length scales of the dipole, ν is the kinematic viscosity and N the Brunt–Väisälä frequency. In practice, we define the horizontal length scale as the dipole radius. It is mainly determined by the size of the flaps, which is fixed in this experimental setup. The dipole translation speed is controlled by the closing speed and initial and final angles of the flaps. For the present experiments these were kept constant. The initial vertical length scale L_{v0} is varied by modifying the height of the aperture in the screen (H) and is defined from particle image velocimetry (PIV) measurements in the vertical plane of symmetry of the dipole as the vertical distance between the point where the velocity is maximum and the point where it is half the maximum.

Measurements of the velocity field were obtained by PIV (FlowMaster 3S, LaVision). The image acquisition is made by a double-frame camera with resolution of 1280×1024 pixels and a 12-bit dynamic range. The pulsed laser sheet was generated with a continuous-beam 7 W Argon laser chopped with an optoacoustic device. The thickness of the light sheet was adjusted to 5 mm at the region of interest. The laser sheet was either on the vertical or on the horizontal symmetry planes and gave access, respectively, to vertical and horizontal velocity fields. In both cases, TiO_2 particles are used as flow seeding. These particles are slightly heavier than the salt-water at the bottom of the tank, but they sediment very slowly (less than 10^{-2} mm s^{-1}) so that, for the time scales used for the PIV shots, they can be reasonably regarded as neutrally buoyant throughout the whole height of the experimental tank. All observations are made after the dipole has crossed the diaphragm, so $t = 0$ is defined when the maximum velocity region at the core of the dipole leaves the screen (t_1 in figure 1). This time origin corresponds for all experiments to 30 s after the flaps are closed.

3. Observations

Two sets of experiments are reported here that correspond to two distinct initial aspect ratios. In the first series (case I) the window height was set to $H = 5.3$ cm, which resulted on an initial vertical length scale of $L_v = 1.5$ cm. The initial control parameters were $F_{h0} = 0.06$, $Re_0 = 131$ and $\alpha_0 = 0.4$. PIV measurements on the horizontal mid-plane (not shown here) demonstrated that the horizontal structure of the dipole can be reasonably described using the Lamb–Chaplygin model and were used to determine the horizontal length scale L_h. Figure 2(a) shows the modulus of the velocity field $|V|$ in the vertical symmetry plane (x, z) of the dipole, at times $t = 5, 50$ and 112 s. The screen position is out of view about 1 cm away from the left edge of the region captured in the images. The corresponding fields of horizontal vorticity ω_h (pointing out of the image plane) are shown in figure 2(b). The two shear layers produced by the moving dipole appear as two stripes of opposite-signed horizontal-vorticity regions on the top and bottom of the core region. At the later stages these sheared regions are inclined forward, surrounding an arrow-shaped region of high velocity (figure 2a). Vertical profiles of the velocity modulus $|V|(z)$ at the x-position of the maximum velocity (figure 3a) show that the vertical width slightly increases whereas the velocity fades away.

In the second set of experiments (case II) the window height was approximately doubled ($H = 10.5$ cm), determining an initial vertical length scale of $L_v = 3.3$ cm. The dipole came out of the screen with a larger initial speed, because a smaller fraction of the energy is lost in the initial adjustment, and the overall evolution was faster. The initial control parameters were $F_{h0} = 0.18$, $Re_0 = 182$ and $\alpha_0 = 1.27$. For the same observation window as in the previous case, the fields of $|V|$ and ω_h shown in
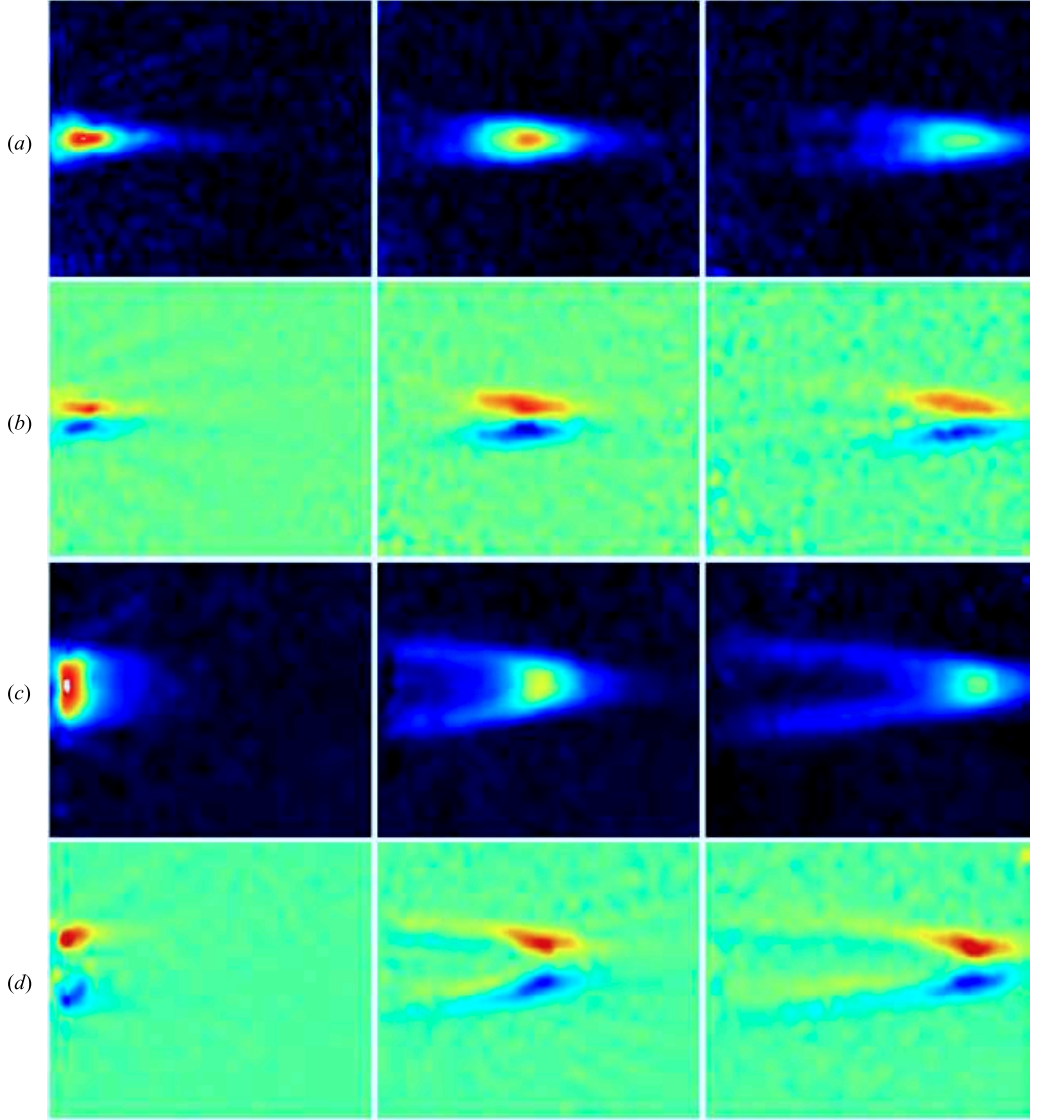
FIGURE 2. Time series of PIV measurements on a vertical cross-section through the dipole symmetry axis. (a) Velocity modulus $|V|$ and (b) horizontal vorticity ω_h for a dipole of case I at times $t = 5, 50$ and $112\,\text{s}$ (from left to right). (c), (d) Analogous fields taken for a dipole of case II at times $t = 0, 35$ and $90\,\text{s}$. Each frame shows an area of $43\,\text{cm}$ in the horizontal (x) direction times $34\,\text{cm}$ in the vertical (z). In (a) and (c) the colourbar of the first frame is used throughout the subsequent frames while in (b) and (d) the colourbar is normalized within each frame.

figures 2(c) and 2(d) were taken at $t = 0, 35$ and $90\,\text{s}$. The analogue profiles of $|V|(z)$ are shown in figure 3(b). Contrary to what was observed in the previous case, the vertical width of the dipole diminishes significantly. The velocity fields in figures 2(c) exhibit a horizontal V-shape, the layers on the top and bottom of the dipole being swept away, generating two 'wakes' in the upper and lower layers where the velocity is horizontal and the vorticity changes sign (see figure 4). The decrease on the vertical length scale is thus caused by the top and bottom layers that are left behind.
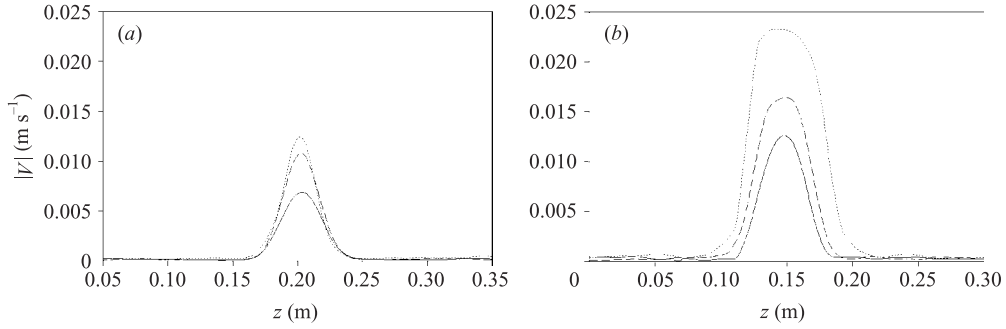
FIGURE 3. Profiles of $|V|(z)$ for: (a) case I at times $t = 5$, 50 and 112 s and (b) case II at times $t = 0$, 35 and 90 s. In each case the profile with highest maximum velocity corresponds to the earliest time. Each profile is obtained by averaging on a 5 mm wide region.
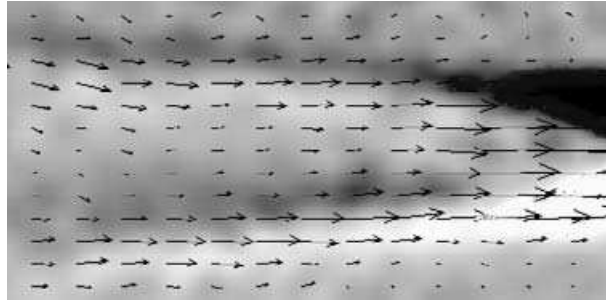

FIGURE 4. Detail of the last frame in figure 2(d) rendered with a contrast-enhancing greyscale. Velocity vectors are also shown. The two layers peeled from the dipole are clearly visible as two quasi-horizontal stripes where vorticity changes sign.
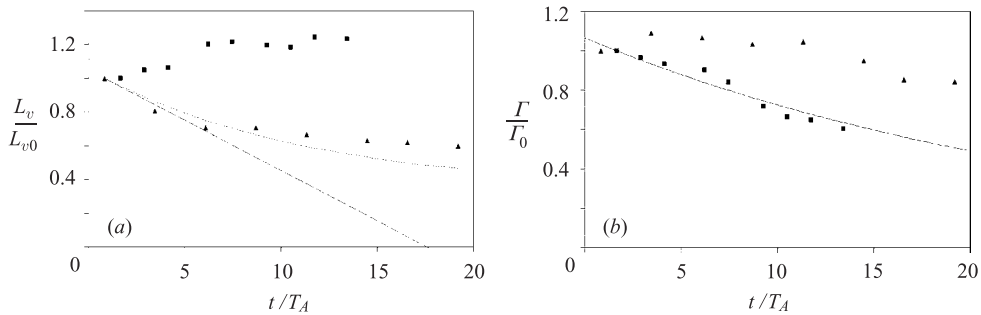

FIGURE 5. Time evolution of (a) the vertical length scale L_v and (b) the circulation of a dipole half, Γ, for both experiments. All curves are normalized to initial values. Time is scaled by the advective time $T_A = L_h/U$. ■, case I; ▲, case II. The constant-thickness model is shown in solid lines. The viscous peel-off model is shown in dashed lines and the dotted line in (a) shows an improvement of this model (see text).

We summarize the observations in figures 5(a) and 5(b) where the time evolution of the vertical length scale L_v and the circulation for one vortex in the dipole Γ are shown. The time axis is rendered non-dimensional using the advective time gauge $T_A = L_{h0}/U_0$. L_v and Γ are normalized by their initial values. In case I the

vertical length scale grows slowly while the circulation decreases, a regime previously observed (see e.g. Flor *et al.* 1995). On the other hand, in case II the vertical length scale decreases while the circulation on the mid-plane remains almost constant, to our knowledge a novel observation.

4. Decay models: viscous peel-off

In case I (thin dipole), if we neglect the slight growth of the thickness, the evolution is described well by the model proposed by Flor *et al.* (1995) in which circulation decreases through vertical diffusion on a time scale $\tau_{ct} \sim \nu^{-1}L_v^2$, whereas the vertical and horizontal structures are assumed frozen with a constant vertical thickness. This constant-thickness diffusion model (solid lines in figure 5) does not contain any adjustable parameter and it predicts remarkably well the circulation decrease observed in case I. This model, however, is not appropriate to describe our second experimental observation where the thickness of the dipole decreases (figure 5a).

In order to give a physical interpretation of this second regime, we reconsider the theoretical framework defined by Riley, Metcalfe & Weissman (1981) and developed in Godoy-Diana & Chomaz (2003), where a scaling analysis of the equations for a stratified viscous fluid in the Boussinesq approximation is conducted: the horizontal velocity is non-dimensionalized by U, the vertical velocity by $U F_v F_h$, the horizontal and vertical length scales by L_h and L_v, the density perturbation by $\rho_0 U^2/gL_v$ and the time scale by L_h/U the horizontal turn-over time. Using the notation $D_h/Dt = \partial/\partial t + \boldsymbol{u}_h \cdot \nabla_h$ for the horizontal Lagrangian derivative, the equations are

$$\frac{D_h \boldsymbol{u}_h}{Dt} + \frac{F_h^2}{\alpha^2} u_z \frac{\partial \boldsymbol{u}_h}{\partial z} = -\nabla_h p + \frac{1}{Re}\left(\nabla_h^2 \boldsymbol{u}_h + \frac{1}{\alpha^2}\frac{\partial^2 \boldsymbol{u}_h}{\partial z^2}\right), \tag{4.1}$$

$$F_h^2\left(\frac{D_h u_z}{Dt} + \frac{F_h^2}{\alpha^2} u_z \frac{\partial u_z}{\partial z}\right) = -\frac{\partial p}{\partial z} - \rho + \frac{F_h^2}{Re}\left(\nabla_h^2 u_z + \frac{1}{\alpha^2}\frac{\partial^2 u_z}{\partial z^2}\right), \tag{4.2}$$

$$\nabla_h \cdot \boldsymbol{u}_h + \frac{F_h^2}{\alpha^2}\frac{\partial u_z}{\partial z} = 0, \tag{4.3}$$

$$\frac{D_h \rho}{Dt} + \frac{F_h^2}{\alpha^2} u_z \frac{\partial \rho}{\partial z} = u_z + \frac{1}{Re\,Sc}\left(\nabla_h^2 \rho + \frac{1}{\alpha^2}\frac{\partial^2 \rho}{\partial z^2}\right), \tag{4.4}$$

where we have used the definitions of the Reynolds $Re = UL_h/\nu$ and Schmidt $Sc = \nu/\kappa$ numbers, the aspect ratio $\alpha = L_v/L_h = F_h/F_v$ and the horizontal $F_h = U/L_h N$ and vertical $F_v = U/L_v N = F_h/\alpha$ Froude numbers. For simplicity in the discussion α will be assumed small so that horizontal diffusion can be neglected compared to vertical diffusion, the extension to the case where this assumption may be relaxed being left to the sagacity of the reader.

Assuming F_h also small, two dominant balances of the horizontal momentum equation (4.1) can be achieved depending on the parameter $R = ReF_h^2$. If $R \gg 1$, vertical transport (second term on the left-hand side of (4.1)) dominates over vertical diffusion. Then the equations are self-similar with respect to N and the vertical length scale imposed by the leading order dynamics is such that $F_v = O(1)$, i.e. $L_v = L_b \equiv U/N$ (Billant & Chomaz 2001). This limit will be used in the final discussion. The present experiments illustrate the other limit $R \ll 1$. In this case, vertical transport terms can be neglected compared to vertical diffusion terms. Thus, the vertical derivative in the horizontal momentum equations appears only in the viscous vertical diffusion and therefore the dominant balance that fixes the vertical length scale is $\alpha^2 Re = 1$. The
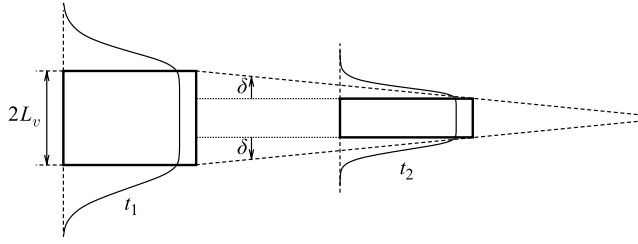
FIGURE 6. Schematic diagram of the two boundary layers during the slim-down regime (see text).

vertical scale

$$L_v = \delta \equiv L_h Re^{-1/2} \tag{4.5}$$

that should appear is then independent of N. The non-dimensional equations in this viscous regime are at leading order

$$\frac{D_h \boldsymbol{u}_h}{Dt} = -\nabla_h p + \frac{\partial^2 \boldsymbol{u}_h}{\partial z^2}, \tag{4.6}$$

$$0 = -\frac{\partial p}{\partial z} - \rho, \tag{4.7}$$

$$\nabla_h \cdot \boldsymbol{u}_h = 0, \tag{4.8}$$

$$\frac{D_h \rho}{Dt} = u_z + \frac{1}{Sc} \frac{\partial^2 \rho}{\partial z^2}. \tag{4.9}$$

These equations have already been introduced by many authors (Riley *et al.* 1981; Lilly 1983; Praud & Fincham 2003). The difference here is that the only hypotheses are $F_h \ll 1$ and $R = ReF_h^2 \ll 1$, the vertical length scale being then imposed by the similarity corresponding to the dominant balance in (4.1) and not by initial or boundary conditions. The determination of the vertical length scale in this viscous stratified regime is to our knowledge a novel result. The horizontal motion is then ruled only by (4.6) and (4.8). These equations resemble the Prandtl equation for the boundary layer over a horizontal plate except that p is not fixed by the external field but should ensure the incompressibility of the horizontal field and that the vertical transport of momentum and the vertical divergence are here negligible.

From the observations of our second set of experiments (figures 2c, d and 3b) we can see that the action of vertical diffusion will be especially important in the horizontal layers that act as boundaries between the moving dipole core and the quiescent fluid over and under it (the high shear regions appearing as dark and light zones in figure 4). In order to model the observed behavior we consider two regimes in time. At the early stages of the evolution, the dipole is sufficiently tall and straight to assume that $\partial \boldsymbol{u}_h / \partial z = 0$ close to the mid-plane. Thus, the horizontal circulation at the mid-plane should be conserved, a feature that corresponds to the experimental observations of case II for times up to $15T_A$ (see figure 5b). The height of the core region around the mid-plane diminishes as the outer layers are slowed down – diffusing momentum to the still regions on the top and bottom of the dipole – until a viscous vertical length scale is reached. This is shown schematically in figure 6. The two 'boundary' layers of thickness δ (as defined in (4.5)) on each side of the

pancake dipole are left behind as the dipole moves.† They peel off vorticity from the pancake dipole and a simple momentum balance predicts that the dimensional vertical scale of the dipole should decrease with time as $L_{v0} - \delta t U/L_h$ until it reaches δ, where L_{v0} is the initial value of L_v. This happens at a time

$$T \sim \frac{L_h}{U} \left(\frac{L_{v0}}{L_h} Re^{1/2} - 1 \right). \tag{4.10}$$

At that time where $\delta \sim L_v$, the evolution becomes purely diffusive as in case I and the thickness of the dipole remains of order δ. The prediction of this *viscous peel-off model* is shown in dashed lines in figure 5: the vertical length scale decreases linearly while the horizontal circulation remains constant. The slope predicted by the model is in good agreement with the initial decrease of L_v in the experiment for case II but it quickly overestimates the evolution at later times. This happens because the model with constant circulation considers inviscid dynamics within the dipole core, which is strictly valid only if L_v/δ is infinitely large and if horizontal viscous dissipation is neglected. In the present experiment, the ratio L_v/δ is about 3 and viscous diffusion affects the evolution of the core layer. Its effect can be simply accounted for by using in the model the experimental data for L_h and Re as functions of time instead of the initial values. This quasi-steady model is in good agreement even for later times as shown by the dotted line in figure 5(*a*).

In summary, when the parameter R is small two types of evolution are possible depending on the initial aspect ratio α_0: either, as in case I of the experiment, the vertical size of the vortex is initially comparable to (or smaller than) δ and it remains so following adiabatically the evolution of δ; or, as in case II, the vertical scale is initially larger than δ and the peel off of viscous layers of thickness δ is observed until $L_v \sim \delta$. In this case the time predicted by (4.10) for the duration of the first regime $T \sim Re^{1/2} L_{v0}/U \sim \alpha_0 Re^{1/2} T_A (\sim 17 T_A)$, where T_A is the advection time L_h/U and α_0 is the initial aspect ratio, compares well with the observed time $T_{exp} \sim 15 T_A$ (estimated from figure 5), in which the vertical scale decreases to the viscous scale $\delta \sim L_h Re^{-1/2}$ and then starts increasing slowly. Accordingly, the horizontal circulation in the mid-plane is first constant and then starts slowly decreasing by diffusion.

5. Discussion and conclusions

A new mechanism responsible for the formation of small-scale vertical structure in strongly stratified fluids has been identified in the present study. This mechanism cooperates with the zigzag instability (Billant & Chomaz 2000*a*) and with the kinematic decorrelation described by Lilly (1983) due to the independent advection of different horizontal layers and it allows us to propose two scenarii for the evolution of strongly stratified pancake turbulence based on the parameter $R = ReF_h^2$. This parameter can also be seen as the squared ratio of the buoyancy length scale $L_b = U/N$ to viscous length scale $\delta = L_h Re^{-1/2}$.

If we consider a strongly stratified flow with R smaller than or equal to order unity (i.e. $\delta \gg L_b$) and initially L_v larger than δ, then the mechanism described here with creation of free 'boundary' layers of thickness δ should occur because there are no forces that counteract the viscous strain force. Through this mechanism the vertical thickness should rapidly decrease to δ on a time scale $\alpha_0 Re^{1/2} T_A$ and

† A similar scaling for Ekman layers was invoked by Chomaz *et al.* (1993) to explain the vertical diffusion in a stratified far wake.

then follow viscous evolution. The flow obeys the Riley *et al.* (1981) leading-order equations:

$$\frac{D_h \boldsymbol{u}_h}{Dt} = -\nabla_h p + \frac{1}{\alpha^2 Re}\frac{\partial^2 \boldsymbol{u}_h}{\partial z^2}, \tag{5.1}$$

$$\nabla_h \cdot \boldsymbol{u}_h = 0, \tag{5.2}$$

equivalent to equations (4.6) and (4.8). Differentiating with respect to z we get

$$\frac{\partial}{\partial t}\frac{\partial \boldsymbol{u}_h}{\partial z} + \boldsymbol{u}_h \cdot \nabla_h \frac{\partial \boldsymbol{u}_h}{\partial z} + \frac{\partial \boldsymbol{u}_h}{\partial z}\cdot\nabla_h \boldsymbol{u}_h = -\nabla_h \frac{\partial p}{\partial z} + \frac{1}{\alpha^2 Re}\frac{\partial^3 \boldsymbol{u}_h}{\partial z^3}. \tag{5.3}$$

The term $(\partial \boldsymbol{u}_h/\partial z)\cdot\nabla_h \boldsymbol{u}_h$ bears some resemblance to the stretching term of the usual unstratified vorticity dynamics – it is analogous to the gradient enhancing term for the advection of a passive scalar (see e.g. Batchelor 1967). This straightforward consideration similar to the ideas of Lilly (1983) and Majda & Grote (1997) explains the increase of the vertical shear on a time scale T_A, the turn-over time of the vortices, due to the evolution of each layer independently, if $L_v \gg \delta$. However, these layers no longer evolve independently when the vertical length scale reaches the viscous scale $L_v \sim \delta$ such that $\alpha^2 Re \sim 1$. At this time viscous effects come into play and limit the decrease of the layer thickness.

In contrast, when $R \gg 1$, i.e. $\delta \ll L_b$, viscous effects are negligible and, even if the initial vertical scale is large, the buoyancy length scale L_b is imposed on a time scale T_A, either through the kinematic mechanism invoked above or through three-dimensional instabilities such as the zigzag instability. In this inviscid regime, once the vertical scale is reduced to the buoyancy length scale, (5.1) and (5.2) (with $Re \to \infty$) should be replaced by the continuous shallow-water equations proposed by Billant & Chomaz (2000b, 2001). The dynamics may escape this attractor if the assumption of large horizontal scale compared to buoyancy length scale (i.e. small horizontal Froude number) is relaxed. Indeed, when the vertical scale is close to L_b the vertical shear may dominate over the stratification and the flow may become unstable to Kelvin–Helmholtz modes that generate small-horizontal scales as observed in recent numerical simulations of Riley & deBruynKops (2003). The turbulence so generated would induce a decrease of the R parameter as a result of the decreasing buoyancy length scale L_b and the increasing viscous length scale δ until, eventually, $R \sim 1$ ($L_b \sim \delta$) and the viscous regime described above would take over. Thus, the final vertical scale is solely determined by viscosity and equals δ.

The late time evolution of strongly stratified flows often observed in laboratory experiments pertains to this final small-R regime. This may explain experimental observations where the vertical length scale has been reported to be independent of the Froude number (or the Brunt–Väisälä frequency) (e.g. Fincham *et al.* 1996; Bonnier *et al.* 2000). We propose that strongly stratified decaying turbulence should ultimately obey a unique scaling law defined by viscosity and independent of the stratification. However, the route to reach this dynamical attractor will vary depending on the initial values of R and the aspect ratio. If now the turbulence were forced and not freely decaying, we may further conjecture that the energy distribution in scale should be determined not only the final viscous attractor, but also the different routes to reach it. A cascade model involving the kinematic effect, the zigzag and Kelvin–Helmholtz instabilities and the viscous decorrelation of layers remains to be formulated.

REFERENCES

BATCHELOR, G. 1967 *An Introduction to Fluid Dynamics.* Cambridge University Press.

BECKERS, M., VERZICCO, R., CLERCX, H. & VAN HEIJST, G. 2001 Dynamics of pancake-like vortices in a stratified fluid: experiments, model and numerical simulations. *J. Fluid Mech.* **433**, 1–27.

BILLANT, P. & CHOMAZ, J. 2000a Experimental evidence for a zigzag instability of a vertical columnar vortex pair in a strongly stratified fluid. *J. Fluid Mech.* **418**, 167–188 (referred to herein as BC).

BILLANT, P. & CHOMAZ, J. 2000b Three dimensional stability of a vertical columnar vortex pair in a strongly stratified fluid. *J. Fluid Mech.* **419**, 65–91.

BILLANT, P. & CHOMAZ, J. 2001 Self-similarity of strongly stratified inviscid flows. *Phys. Fluids* **13**, 1645–1651.

BONNIER, M., EIFF, O. & BONNETON, P. 2000 On the density structure of far-wake vortices in a stratified fluid. *Dyn. Atmos. Oceans* **31**, 117–137.

BOUBNOV, B., GLEDZER, E. & HOPFINGER, E. 1995 Stratified circular couette flow: instability and flow regimes. *J. Fluid Mech.* **292**, 333–358.

CHOMAZ, J., BONNETON, P., BUTET, A. & HOPFINGER, E. 1993 Vertical diffusion of the far wake of a sphere moving in a stratified fluid. *Phys. Fluids* A **5**, 2799–2806.

FINCHAM, A., MAXWORTHY, T. & SPEDDING, G. 1996 Energy dissipation and vortex structure in freely decaying, stratified grid turbulence. *Dyn. Atmos. Oceans* **23**, 155–169.

FLOR, J., VAN HEIJST, G. & DELFOS, R. 1995 Decay of dipolar vortex structures in a stratified fluid. *Phys. Fluids* **7**, 374–383.

GODEFERD, F. & STAQUET, C. 2003 Statistical modelling and direct numerical simulations of decaying stably stratified turbulence. part 2. large-scale and small-scale anisotropy. *J. Fluid Mech.* **486**, 115–159.

GODOY-DIANA, R. & CHOMAZ, J. 2003 Effect of the schmidt number on the diffusion of axisymmetric pancake vortices in a stratified fluid. *Phys. Fluids* **15**, 1058–1064.

HERRING, J. & MÉTAIS, O. 1989 Numerical experiments in forced stably stratified turbulence. *J. Fluid Mech.* **202**, 97–115.

HOLFORD, J. & LINDEN, P. 1999 Turbulent mixing in a stratified fluid. *Dyn. Atmos. Oceans* **30**, 173–198.

KIMURA, Y. & HERRING, J. 1996 Diffusion in stably stratified turbulence. *J. Fluid Mech.* **328**, 253–269.

LILLY, D. 1983 Stratified turbulence and the mesoscale variability of the atmosphere. *J. Atmos. Sci.* **40**, 749–761.

LINDBORG, E. 2002 Strongly stratified turbulence: A special type of motion. In *Advances in Turbulence IX. Proc. Ninth European Turbulence Conference* (ed. I. P. Castro, P. E. Hancock & T. G. Thomas), pp. 435–442. CIMNE, Barcelona.

MAJDA, A. & GROTE, M. 1997 Model dynamics and vertical collapse in decaying strongly stratified flows. *Phys. Fluids* **9**, 2932–2940.

PARK, Y.-G., WHITEHEAD, J. & GNANADESKIAN, A. 1994 Turbulent mixing in stratified fluids: layer formation and energetics. *J. Fluid Mech.* **279**, 279–311.

PRAUD, O. & FINCHAM, A. 2003 The structure and dynamics of stratified dipolar vortices. *J. Fluid Mech.* (submitted).

RILEY, J. & DEBRUYNKOPS, S. 2003 Dynamics of turbulence strongly influenced by buoyancy. *Phys. Fluids* **15**, 2047–2059.

RILEY, J. & LELONG, M. 2000 Fluid motions in the presence of strong stable stratification. *Annu. Rev. Fluid Mech.* **32**, 613–657.

RILEY, J., METCALFE, R. & WEISSMAN, M. 1981 Direct numerical simulations of homogeneous turbulence in density stratified fluids. In *Proc. AIP Conf. on Nonlinear Properties of Internal Waves* (ed. B. West), pp. 79–112. La Jolla Institute.

SPEDDING, G. 2002 Vertical structure in stratified wakes with high initial froude number. *J. Fluid Mech.* **454**, 71–112.

SPEDDING, G., BROWAND, F. & FINCHAM, A. 1996 Turbulence, similarity scaling and vortex geometry in the wake of a towed sphere in a stably-stratified fluid. *J. Fluid Mech.* **314**, 53–103.